Spatially Resolving the Quasar Broad Emission Line Region

GRAVITY Collaboration

Roberto Abuter [8]
Matteo Accardo [8]
Tobias Adler [3]
António Amorim [6]
Narsireddy Anugu [7, 29, 30]
Gerardo Ávila [8]
Michi Bauböck [1]
Myriam Benisty [5, 12]
Jean-Philippe Berger [5]
Joachim M. Bestenlehner [22, 3]
Hervé Beust [5]
Nicolas Blind [9]
Mickaël Bonnefoy [5]
Henri Bonnet [8]
Pierre Bourget [8]
Jérôme Bouvier [5]
Wolfgang Brandner [3]
Roland Brast [8]
Alexander Buron [1]
Leonard Burtscher [14]
Faustine Cantalloube [3]
Alessio Caratti o Garatti [16, 3]
Paola Caselli [1]
Frédéric Cassaing [10]
Frédéric Chapron [2]
Benjamin Charnay [2]
Élodie Choquet [37]
Yann Clénet [2]
Claude Collin [2]
Vincent Coudé du Foresto [2]
Ric Davies [1]
Casey Deen [1]
Françoise Delplancke-Ströbele [8]
Roderick Dembet [8]
Frédéric Derie [8]
Willem-Jan de Wit [8]
Jason Dexter [1]
Tim de Zeeuw [1, 14]
Catherine Dougados [5]
Guillaume Dubus [5]
Gilles Duvert [5]
Monica Ebert [3]
Andreas Eckart [4, 13]
Frank Eisenhauer [1]
Michael Esselborn [8]
Fabio Eupen [4]
Pierre Fédou [2]
Miguel C. Ferreira [6]
Gert Finger [8]
Natascha M. Förster Schreiber [1]
Feng Gao [1]
César Enrique García Dabó [8]
Rebeca Garcia Lopez [16, 3]
Paulo J. V. Garcia [7]
Éric Gendron [2]
Reinhard Genzel [1, 15]
Ortwin Gerhard [1]

Juan Pablo Gil [8]
Stefan Gillessen [1]
Frédéric Gonté [8]
Paulo Gordo [6]
Damien Gratadour [2]
Alexandra Greenbaum [40]
Rebekka Grellmann [4]
Ulrich Grözinger [3]
Patricia Guajardo [8]
Sylvain Guieu [5]
Maryam Habibi [1]
Pierre Haguenauer [8]
Oliver Hans [1]
Xavier Haubois [8]
Marcus Haug [8]
Frank Haußmann [1]
Thomas Henning [3]
Stefan Hippler [3]
Sebastian F. Hönig [27]
Matthew Horrobin [4]
Armin Huber [3]
Zoltan Hubert [5]
Norbert Hubin [8]
Christian A. Hummel [8]
Gerd Jakob [8]
Annemieke Janssen [36]
Alejandra Jimenez Rosales [1]
Lieselotte Jochum [8]
Laurent Jocou [5]
Jens Kammerer [8, 41]
Martina Karl [20, 21]
Andreas Kaufer [8]
Stefan Kellner [1]
Sarah Kendrew [11, 3]
Lothar Kern [8]
Pierre Kervella [2]
Mario Kiekebusch [8]
Makoto Kishimoto [31]
Lucia Klarmann [3]
Ralf Klein [3]
Rainer Köhler [3]
Yitping Kok [1]
Johann Kolb [8]
Maria Koutoulaki [16, 19, 3, 8]
Martin Kulas [3]
Lucas Labadie [4]
Sylvestre Lacour [2, 8]
Anne-Marie Lagrange [5]
Vincent Lapeyrère [2]
Werner Laun [3]
Bernard Lazareff [5]
Jean-Baptiste Le Bouquin [5]
Pierre Léna [2]
Rainer Lenzen [3]
Samuel Lévêque [8]
Chien-Cheng Lin [3, 18]
Magdalena Lippa [1]
Dieter Lutz [1]
Yves Magnard [5]

Anne-Lise Maire [23, 3]
Leander Mehrgan [8]
Antoine Mérand [8]
Florentin Millour [37]
Paul Mollière [3]
Thibaut Moulin [5]
André Müller [3]
Eric Müller [8, 3]
Friedrich Müller [3]
Hagai Netzer [32]
Udo Neumann [3]
Mathias Nowak [2]
Sylvain Oberti [8]
Thomas Ott [1]
Laurent Pallanca [8]
Johana Panduro [3]
Luca Pasquini [8]
Thibaut Paumard [2]
Isabelle Percheron [8]
Karine Perraut [5]
Guy Perrin [2]
Bradley M. Peterson [24, 25, 26]
Pierre-Olivier Petrucci [5]
Andreas Pflüger [1]
Oliver Pfuhl [8]
Than Phan Duc [8]
Jaime E. Pineda [1]
Philipp M. Plewa [1]
Dan Popovic [8]
Jörg-Uwe Pott [3]
Almudena Prieto [39]
Laurent Pueyo [11]
Sebastian Rabien [1]
Andrés Ramírez [8]
José Ricardo Ramos [3]
Christian Rau [1]
Tom Ray [16]
Miguel Riquelme [8]
Gustavo Rodríguez-Coira [2]
Ralf-Rainer Rohloff [3]
Daniel Rouan [2]
Gérard Rousset [2]
Joel Sanchez-Bermudez [3, 17]
Marc Schartmann [1, 33, 34]
Silvia Scheithauer [3]
Markus Schöller [8]
Nicolas Schuhler [8]
Dominique Segura-Cox [1]
Jinyi Shangguan [1]
Thomas T. Shimizu [1]
Jason Spyromilio [8]
Amiel Sternberg [1, 32]
Matthias Raphael Stock [21]
Odele Straub [1, 2]
Christian Straubmeier [4]
Eckhard Sturm [1]
Marcos Suárez Valles [8]
Linda J. Tacconi [1]
Wing-Fai Thi [1]

Konrad R. W. Tristram [8]
Javier J. Valenzuela [8]
Roy van Boekel [3]
Ewine F. van Dishoeck [14]
Pierre Vermot [2]
Frédéric Vincent [2]
Sebastiano von Fellenberg [1]
Idel Waisberg [1]
Jason J. Wang [28]
Imke Wank [4]
Johannes Weber [1]
Gerd Weigelt [13]
Felix Widmann [1]
Ekkehard Wieprecht [1]
Michael Wiest [4]
Erich Wiezorrek [1]
Markus Wittkowski [8]
Julien Woillez [8]
Burkhard Wolff [8]
Pengqian Yang [3,35]
Senol Yazici [1,4]
Denis Ziegler [2]
Gérard Zins [8]

[1] Max Planck Institute for Extraterrestrial Physics, Garching, Germany
[2] LESIA, Observatoire de Paris, Université PSL, CNRS, Sorbonne Université, Université de Paris, Meudon, France
[3] Max-Planck-Institut für Astronomie, Heidelberg, Germany
[4] I Physikalisches Institut, Universität zu Köln, Germany
[5] Univ. Grenoble Alpes, CNRS, IPAG, Grenoble, France
[6] CENTRA and Universidade de Lisboa – Faculdade de Ciências, Lisboa, Portugal
[7] CENTRA and Universidade do Porto – Faculdade de Engenharia, Porto, Portugal
[8] ESO
[9] Observatoire de Genève, Université de Genève, Versoix, Switzerland
[10] DOTA, ONERA, Université Paris-Saclay, Châtillon, France
[11] European Space Agency, Space Telescope Science Institute, Baltimore, USA
[12] Unidad Mixta Internacional Franco-Chilena de Astronomía (CNRS UMI 3386), Departamento de Astronomía, Universidad de Chile, Las Condes, Santiago, Chile
[13] Max Planck Institute for Radio Astronomy, Bonn, Germany
[14] Sterrewacht Leiden, Leiden University, Leiden, the Netherlands
[15] Department of Physics, Le Conte Hall, University of California, Berkeley, USA
[16] Dublin Institute for Advanced Studies, Dublin, Ireland
[17] Instituto de Astronomía, Universidad Nacional Autónoma de México, Ciudad de México, Mexico
[18] Institute for Astronomy, University of Hawai'i, Honolulu, USA
[19] School of Physics, University College Dublin, Ireland
[20] Max Planck Institute for Physics, Munich, Germany
[21] TUM Department of Physics, Technical University of Munich, Garching, Germany
[22] Department of Physics and Astronomy, University of Sheffield, UK
[23] STAR Institute, Liège, Belgium
[24] Department of Astronomy, The Ohio State University, Columbus, USA
[25] Center for Cosmology and AstroParticle Physics, The Ohio State University, Columbus, USA
[26] Space Telescope Science Institute, Baltimore, USA
[27] School of Physics & Astronomy, University of Southampton, UK
[28] Department of Astronomy, California Institute of Technology, Pasadena, USA
[29] Steward Observatory, Department of Astronomy, University of Arizona, Tucson, USA
[30] University of Exeter, School of Physics and Astronomy, Exeter, UK
[31] Kyoto Sangyo University, Department of Astrophysics and Atmospheric Sciences, Japan
[32] School of Physics and Astronomy, Tel Aviv University, Israel
[33] Excellence Cluster Origins, Ludwig-Maximilians-Universität München, Garching, Germany
[34] Universitäts-Sternwarte München, Munich, Germany
[35] Shanghai Institute of Optics and Fine Mechanics, Chinese Academy of Sciences, China
[36] NOVA Optical Infrared Instrumentation Group at ASTRON, Dwingeloo, the Netherlands
[37] Aix Marseille Univ, CNRS, CNES, LAM, France
[38] Observatoire de la Côte d'Azur Lagrange, Boulevard de l'Observatoire, Nice, France
[39] Instituto de Astrofísica de Canarias, La Laguna, Spain
[40] University of Michigan Department of Astronomy, Ann Arbor, USA
[41] Research School of Astronomy & Astrophysics, Australian National University, Canberra, Australia

The angular resolution of the Very Large Telescope Interferometer (VLTI) and the excellent sensitivity of GRAVITY have led to the first detection of spatially resolved kinematics of high velocity atomic gas near an accreting supermassive black hole, revealing rotation on sub-parsec scales in the quasar 3C 273 at a distance of 550 Mpc. The observations can be explained as the result of circular orbits in a thick disc configuration around a 300 million solar mass black hole. Within an ongoing Large Programme, this capability will be used to study the kinematics of atomic gas and its relation to hot dust in a sample of quasars and Seyfert galaxies. We will measure a new radius-luminosity relation from spatially resolved data and test the current methods used to measure black hole mass in large surveys.

Introduction

Emission lines of atomic gas velocity-broadened to widths of 3000–10 000 km s⁻¹ are a hallmark of quasars and are thought to trace the gravitational potential of the central supermassive black hole. Despite decades of study their physical origin remains unclear. The observed properties can be explained by emission from discrete, collapsed clouds or high-density regions of a continuous medium. The gas may be part of the inflow feeding the black hole or a continuous equatorial outflow. Assuming a gravitational origin, line widths combined with a measurement of the emission region size provide an estimate of the black hole mass.

Extensive monitoring campaigns use light echoes in a technique called reverberation mapping to measure the emission size, with ongoing work expanding the sample size from tens (Kaspi et al., 2000; Peterson et al., 2004) to hundreds (Du et al., 2016; Grier et al., 2017). The key result of these studies is that the size of the emitting region increases with
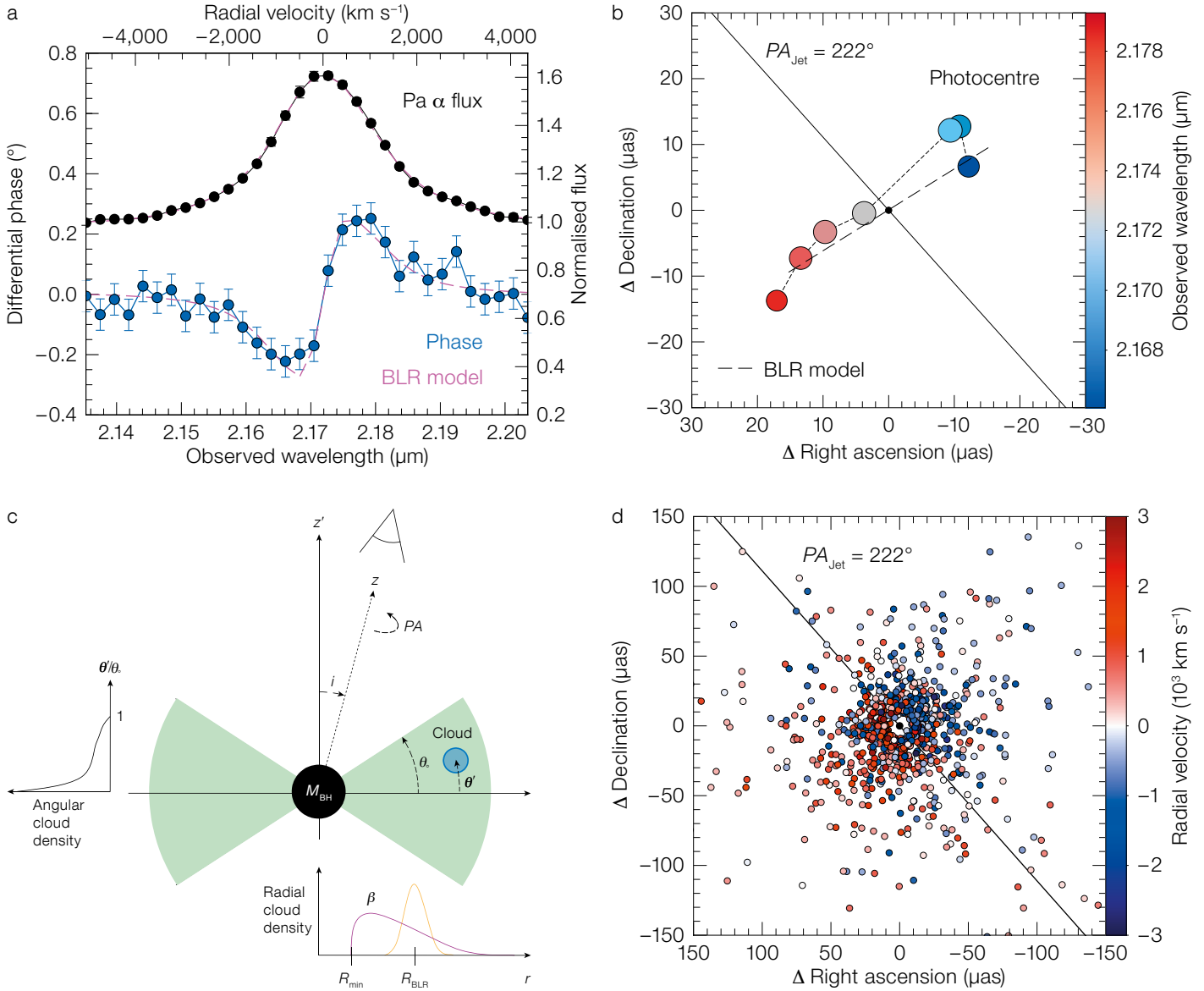
Figure 1. GRAVITY spatially resolves the broad emission line kinematics of 3C 273. (a) Paα line profile (black) and averaged differential phase (blue), showing non-zero phases and a change of sign across the broad emission line. (b) Photocentre positions measured at each line channel, showing a clear separation between red and blue which corresponds to a velocity gradient at a position angle perpendicular t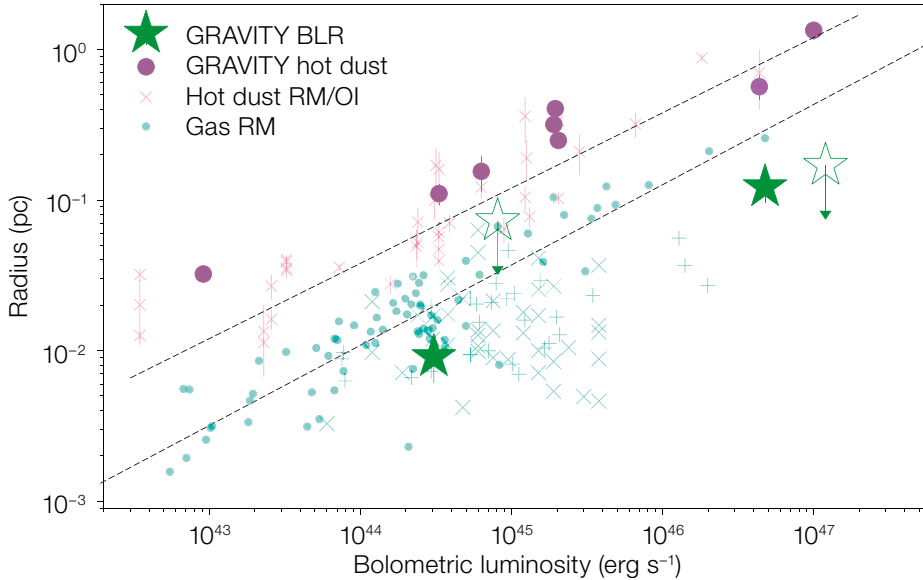o the large-scale radio jet of 3C 273 (black line). This is the result of net ordered rotation of the line-emitting gas. By comparing a kinematic model of the emission region (c) to GRAVITY data, we find that a thick disc configuration viewed at low inclination best explains the data (d). The model also provides estimates of the mean emission radius and central black hole mass. Adapted from GRAVITY Collaboration (2018).

luminosity, roughly as $R \sim L^{1/2}$. That relationship can be understood as atomic gas emission being produced under optimal photoionisation conditions (constant received flux). This radius-luminosity relation allows "secondary" methods for estimating black hole masses using a single optical spectrum (replacing long campaigns to measure R via an estimate based on L). Secondary methods so far provide all available active galactic nucleus (AGN) black hole mass measurements in large samples and out to high redshift.

Interferometry provides an independent method for spatially resolving AGN central engines. The key components of AGN are small on the sky, at micro- to milli-arcsecond scales, requiring long baselines at the VLTI and Keck Interferometer. AGN are also relatively faint sources, so far only detected in optical interferometry with 8–10-metre-class telescopes and instrumentation with excellent sensitivity. Continuum measurements with the Keck Interferometer (for example, Kishimoto et al., 2011) and the Astronomical Multi-BEam combineR (AMBER) on the VLTI (Weigelt et al., 2012) provide information about hot dust surrounding the nucleus. The broad line region (BLR) is even smaller (angular size < 0.1 milliarcseconds [mas]) and is impossible to resolve in standard

Figure 2. AGN radius-luminosity relationships measured for hot dust and atomic gas. The hot dust measurements include our new GRAVITY results (purple solid circles; see GRAVITY Collaboration, 2019a), as well as those from previous observations. For atomic gas, we have detected velocity gradients and measured the emission region size for the quasar 3C 273 (GRAVITY Collaboration, 2018) with another detection and upper limits in deep integrations for two other sources. With an ongoing large programme, we aim to expand the sample to roughly 10 AGN spanning four orders of magnitude in luminosity. The results can be compared to the large scatter found in reverberation mapping samples (different samples as smaller symbols) and to the $R \sim L^{0.5}$ relations found for both dust and atomic gas.

imaging, even with the VLTI. Instead, we can study its kinematics by measuring the photocentre shift of the atomic gas relative to the hot dust, as a function of wavelength (or velocity) across the emission line. The photocentre shift results in a small differential phase signal ≲ 1 degree (Rakshit et al., 2015) whose detection requires high sensitivity and deep integrations. This is now possible with GRAVITY.

A case study in 3C 273

We observed 3C 273 with GRAVITY using the four Unit Telescopes (UTs) over eight nights between July 2017 and May 2018, with a total on-source integration time of 8 hours. By combining the data from all epochs, we measure the interferometric phase with a precision of ~ 0.1–0.2 degrees per baseline. An average of three of the six baselines shows the detection of an S-shaped phase signal, corresponding to a spatially resolved velocity gradient across the otherwise featureless broad Paα emission line (Figure 1a). From the phase data, we fit for a model-independent photocentre position at wavelength channels where the line emission is strong. We find a clear separation between blue and red channels (a velocity gradient, Figure 1b), with an orientation perpendicular to the large-scale radio jet. This demonstrates net rotation of the line emission region. The photocentre positions are measured with a typical precision of 5 μas per channel.

By adopting a kinematic model of the Paα emission region as a collection of orbiting gas clouds (following Pancoast et al., 2014 and Rakshit et al., 2015), we measure physical properties of the gas distribution and black hole. The data are consistent with a thick disc (opening angle of 45^{+9}_{-6} degrees) in Keplerian rotation around a supermassive black hole of $1.5–4.1 \times 10^8$ $M_\odot$. The inclination and position angles agree with those inferred for the radio jet. The measured mean emission radius of $R_{BLR} = 0.12 \pm 0.03$ pc (at an angular diameter distance of 548 Mpc) is a factor of about two smaller than reported in earlier RM studies (Kaspi et al., 2000; Peterson et al., 2004) although it is consistent with a recent one (Zhang et al., 2019). This first result supports the fundamental assumptions used in reverberation mapping and the secondary methods used to measure black hole mass. For more details, see GRAVITY Collaboration (2018).

Outlook

With an approved large programme we are carrying out observations of ~ 10 sources over the next two years, spanning four orders of magnitude in AGN luminosity. The data will provide information on the dominant kinematics and the degree of ordered motion in atomic gas in the broad emission line region, helping us to address the following questions: are the line widths pri-

marily set by rotation in the black hole gravitational potential, or by polar outflow driven by radiation pressure? And is the velocity structure well ordered or randomised?

By modelling the line profile and differential phase data, we will measure the emission region size and construct a new radius-luminosity relationship. Our results can be compared with those obtained independently from reverberation techniques and used to constrain the physical origin of the atomic gas. We will also study the connection of the atomic gas to that of the hot dust continuum which we obtain using the same data (for example, GRAVITY Collaboration, 2019a & b). The angular size of both the hot dust and the atomic gas scales with optical flux, which makes interferometry well suited for studying luminous quasars like 3C 273 as well as nearby Seyfert galaxies. A future upgrade to the sensitivity of GRAVITY could further obtain kinematics, broad emission line region size, and black hole mass estimates for large samples out to a redshift $z \sim 2$.

References

Peterson, B. M. et al. 2004, ApJ, 613, 682
Kaspi, S. et al. 2000, ApJ, 533, 631
Rakshit, S. et al. 2015, MNRAS, 447, 2420

GRAVITY Collaboration 2018, Nature, 563, 657
GRAVITY Collaboration 2019a, submitted to A&A, arXiv:1910.00593
GRAVITY Collaboration 2019b, submitted to A&A
Bentz, M. C. et al. 2013, ApJ, 767, 149
Du, P. et al. 2018, ApJ, 856, 6
Grier, C. J. et al. 2017, ApJ, 851, 21
Pancoast, A. et al. 2008, MNRAS, 445, 3073
Kishimoto, M. et al. 2011, A&A, 527, 121
Weigelt, G. et al. 2012, A&A Letters, 451, 9
Zhang, Z.-X. et al. 2019, ApJ, 876, 49

An Image of the Dust Sublimation Region in the Nucleus of NGC 1068

GRAVITY Collaboration (see page 20)

The superb resolution of the Very Large Telescope Interferometer (VLTI) and the unrivalled sensitivity of GRAVITY have allowed us to reconstruct the first detailed image of the dust sublimation region in an active galaxy. In the nearby archetypal Seyfert 2 galaxy NGC 1068, the 2 µm continuum emission traces a highly inclined thin ring-like structure with a radius of 0.24 pc. The observed morphology challenges the picture of a geometrically and optically thick torus.

Introduction

NGC 1068 is one of the best studied nearby active galactic nuclei (AGN), in which accretion onto a central super-massive black hole contributes a signifi-cant fraction of the galaxy's total luminos-ity. The observation of broad polarised emission lines by Antonucci & Miller (1985) in the nucleus of this Seyfert gal-axy was central to the development of the unified model that explains the differ-ences between Seyfert 1 and Seyfert 2 objects as being due to the presence of a nuclear equatorial structure that both obscures and scatters the central emis-sion depending on the line of sight.

Since the first seminal paper addressing its physical properties (Krolik & Begelman, 1988), and following numerous observa-tions at many different wavelengths, the "torus" concept has evolved and been modified considerably. At the same time, increases in computational power have facilitated detailed modelling of clumpy torus structures. Such models are consistent with the near- to mid-infrared spectral energy distribution as well as dust reverberation measurements. Observations of almost two dozen galaxies using the MID-infrared Interfero-metric instrument (MIDI) on the VLTI have resolved the 1–3 pc scales where warm dust is responsible for the mid-infrared continuum (Burtscher et al., 2013 and ref-erences therein). However, measuring the size of the small (< 1 pc) region con-taining hot dust that emits at near-infra-red wavelengths has been possible in very few galaxies. Also, until GRAVITY observed NGC 1068, there were no data showing spatial structure in this dust sub-limation region.

Observations and Image Reconstruction

Data on NGC 1068 were obtained in November and December 2018 using GRAVITY and the four 8-metre UTs.

Under superb conditions, with seeing ~ 0.5 arcseconds and a coherence time of up to 13 ms, it was possible to fringe-track on the nucleus of NGC 1068 despite its large size and moderate brightness. The data obtained were of excellent quality, with typically < 1% visi-bility and closure-phase accuracy. The wealth of information provided by the six VLTI baselines has enabled us to recon-struct a *K*-band image based on the obtained closure phases and visibilities with 3-milliarcsecond (mas) resolution.

We used the publicly available Multi-aperture image Reconstruction Algorithm (MiRA; Thiébaut, 2008) to generate the image shown in Figure 1, which contains a total flux of 155 mJy. The structures present are robust, having been repro-duced consistently over a wide variety of parameter settings, and with a signal level much higher than that expected for spurious sources. Full details are in GRAVITY Collaboration (2019).

A new view of NGC 1068

The image in Figure 1 is dominated by knots of continuum arranged in a ring around a central hole, with the south-western side about a factor of two brighter than the north-eastern side. Fitting an